HHS Public Access

Author manuscript

Biochim Biophys Acta Biomembr. Author manuscript; available in PMC 2019 May 01.

Published in final edited form as:

Biochim Biophys Acta Biomembr. 2018 May ; 1860(5): 1179–1186. doi:10.1016/j.bbamem.2018.01.020.

THREONINE 67 IS A KEY COMPONENT IN THE COUPLING OF THE NSS AMINO ACID TRANSPORTER KAAT1.

M. Giovanola[a], **A. Vollero**[b,@], **R. Cinquetti**[b], **E. Bossi**[b], **L.R. Forrest**[c], **E. Di Cairano**[a], and **M. Castagna**[a]

[a]Department of Pharmacological and Biomolecular Sciences, Università degli Studi di Milano, Via Trentacoste 2, 20134, Milano, Italy.

[b]Department of Biotechnology and Life Sciences, University of Insubria, Via J.H. Dunant 3, 21100, Varese, Italy.

[c]Computational Structural Biology Section, NIH NINDS, 35 Convent Drive, Bethesda MD 20892-3761, USA

Abstract

The crystallizations of the prokaryotic LeuT and of the eukaryotic DAT and SERT transporters represent important steps forward in the comprehension of the molecular physiology of Neurotransmitter:Sodium Symporters, although the molecular determinants of the coupling mechanism and of ion selectivity still remain to be fully elucidated. The insect NSS homologue KAAT1 exhibits unusual physiological features, such as the ability to use K^+ as the driver ion, weak chloride dependence, and the ability of the driver ion to influence the substrate selectivity; these characteristics can help to define the molecular determinants of NSS function. Two non-conserved residues are present in the putative sodium binding sites of KAAT1: Ala 66, corresponding to Gly 20 in the Na2 site of LeuT, and Ser 68, corresponding to Ala 22 in the Na1 site. Thr 67 appears also to be significant since it is not conserved among NSS members, is present as threonine only in KAAT1 and in the paralogue CAATCH1 and, according to LeuT structure, is close to the amino acid binding site. Mutants of these residues were functionally characterized in *Xenopus* oocytes. The T67Y mutant exhibited uptake activity comparable to that of the wild type, but fully chloride-independent and with enhanced stereoselectivity. Interestingly, although dependent on the presence of sodium, the mutant showed reduced transport-associated currents, indicating uncoupling of the driver ion and amino acid fluxes. Thr 67 therefore appears to be a key component in the coupling mechanism, participating in a network that influences the cotransport of Na^+ and the amino acid.

Keywords

NSS family; structure-function analysis; coupling mechanism; amino acid uptake; ion selectivity; Xenopus laevis oocytes; homology model

Corresponding author: Michela Castagna, Department of Pharmacological and Biomolecular Sciences, Università degli Studi di Milano, Via Trentacoste 2, 20134 Milano, Italy, Tel: +39 0250315808, Fax: +39 0250315813, Michela.Castagna@unimi.it.
[@]Present address: Molecular Cardiology, IRCCS Fondazione Salvatore Maugeri, Via S. Maugeri 10, 27100, Pavia, Italy.

INTRODUCTION

NSS family members comprise neurotransmitter, amino acid, and osmolyte transporters driven by the sodium gradient. Originally classified as uniformly chloride dependent, it is now known that these proteins range from almost completely chloride dependent (typically neurotransmitter transporters), to independent (for all bacterial proteins), with weak dependence exhibited by some eukaryotic nutrient transporters [1–6].

In the first structural prototype of the family LeuT [7], residues from TM 7, 8, and from the unwound regions of TM1 and 6, were shown to contribute to the structural organization of sodium binding sites Na1 and Na2. These ion binding sites are conserved in the recently reported crystal structures of the *Drosophila* dopamine transporter DAT_{cryst} and the human serotonin transporter SERT [8–11]. In the Na1 binding site, the organic substrate coordinates the sodium ion, specifically through its carboxyl group; in DAT_{cryst} Asp 46 substitutes the substrate carboxyl group, coordinating Na^+ through a water molecule. Na2 is less conserved among NSS members but is highly conserved, from a structural point of view, in the FIRL fold family [12] that groups transporters of distant unrelated families sharing the LeuT fold (*Five transmembrane-helix Inverted-topology Repeat, LeuT-like*) [12–14].

The chloride binding site in SERT and in the GABA transporter GAT1 was identified in 2007 [15,16]. Quite interestingly, this site was found to involve some of the same residues as the Na1 site, which, in turn, shares residues with the leucine binding site of LeuT, highlighting the “intimate contact” between driving and driven substrates that enables the transport process [17]. According to these findings, $Cl^–$-independence of the prokaryotic NSS would be achieved through the presence of a negative charge provided by an acidic residue (Glu 290, LeuT numbering) located in the position occupied by a chloride ion in $Cl^–$-dependent transporters. Mutagenesis studies in the bacterial homologues TnaT and LeuT [18,19], together with the chloride binding site described in DAT and in SERT crystal structures [8,11], confirmed this hypothesis.

KAAT1 is a neutral amino acid transporter belonging to the NSS family that shows a unique ion dependence: it is activated by Na^+, K^+, and by Li^+ [20], and is weakly chloride dependent [2]. Even its amino acid selectivity shows peculiarities, since it is determined by the driving ion [21]. The ability to interact with potassium as driving ion was initially identified only in KAAT1 and in the paralogous CAATCH1 [22], but was subsequently described also for other nutrient amino acid transporters (NATs) from the insect class [3]. K^+ exerts a different role in other members of the NSS family: in SERT, binding of this cation facilitates reorientation from the inward facing conformation after substrate release into the cytoplasm [23] and transition metal ion FRET has shown that K^+ inhibits Na^+ and substrate binding in LeuT, possibly by binding to an outward-closed conformation of the transporter [24]. So far, only insect transporters like KAAT1 and CAATCH1 have been demonstrated to be able to perform the transport process in the presence of an inward-directed K^+ gradient [3,25].

Interaction with Li^+ is also common in NSS members: in GAT1 and DAT lithium can bind to the Na2 site, eliciting pre-steady state and leak currents, but it is not exploitable as a driver

ion [26,27]. A Li^+ gradient can, however, be used to drive amino acid uptake by KAAT1, CAATCH1, and the mammalian and fish B^0AT1 transporters [4,20,22,28]. The chloride dependence of KAAT1 is only partial since the protein is able to work in the absence of chloride with a transport activity ranging from 50 to 80% of the control, depending on the transported amino acid [2]. This behavior has been observed also in other transporters [1,2,4,5,6], although the mouse orthologue of B^0AT1 gave controversial results [28,29]. In KAAT1 the corresponding position of LeuT Glu 290 is occupied by a neutral polar residue as found in $Cl^–$-dependent proteins. The relative $Cl^–$-independence of KAAT1 uptake could be attributed to the presence, close to the putative chloride binding site, of an aspartate (Asp 338 KAAT1 numbering), which could partially contribute to the required negative charge. However, other $Cl^–$-independent neutral amino acid transporters (mammalian B^0AT1 and B^0AT2, IMINO, and others) do not appear to have such negative residue in the adjacent regions of the site. Moreover, Asp 338 in KAAT1 has been demonstrated to be involved in the interaction with K^+ and in the spatial organization of the cation binding site and of the permeation pathway [30,31]. In addition to Asp 338, sequence comparisons highlight two non-conserved residues in the putative sodium binding sites of KAAT1: Ala 66, corresponding to Gly 20 in the Na2 site of LeuT, and Ser 68, corresponding to Ala 22 in the Na1 site (Fig. 1). The bridging residue Thr 67 also appears to be significant since it is not conserved among NSS members, it is present as threonine only in KAAT1 and CAATCH1 and, its equivalent in LeuT (Asn 21) is close to the organic substrate. However, it is not clear which of these residues is responsible for the unusual physiological features of KAAT1. Therefore, to help elucidate the molecular determinants of ion interaction and coupling mechanism in the NSS family, we performed a mutagenesis-based analysis of the role exerted by Ala 66, Thr 67 and Ser 68 in KAAT1 function.

MATERIAL AND METHODS

Mutagenesis

KAAT1 mutants were obtained by PCR using high fidelity DNA polymerase *Pfu* (Promega) and the following primers:

A66G: CGAATTCTTGATGTCCTGCATCGGTACATCCGTCGGTTTGGG

T67G: GATGTCCTGCATCGCTGGATCCGTCGGTTTGGGTAAC

T67Y: GTCCTGCATCGCTTACTCCGTCGGTTTGGGTAACGTGTGG

S68A: GTCCTGCATCGCTACAGCCGTCGGTTTGGGTAACG

DNA sequencing confirmed the mutations.

Oocyte harvesting and selection

Oocytes were obtained from adult female *X. laevis* frogs and manually defolliculated after treatment with 1 mg/ml Collagenase A (Roche, Germany) for 30–40 min at RT in Ca^{++}-free ORII medium (82.5 mM NaCl, 2 mM KCl, 1 mM $MgCl_2$, 5 mM HEPES/Tris, pH 7.5). Healthy V–VI stadium oocytes [32] were then selected for injection and maintained at 16 °C in Barth's solution (88 mM NaCl, 1 mM KCl, 0.82 mM $MgSO_4$, 0.41 mM $CaCl_2$, 0.33 mM $Ca(NO_3)_2$, 2.4 mM $NaHCO_3$, 10 mM HEPES/Tris, pH 7.5) supplemented with 50 mg/l

gentamicin sulfate and 2.5 mM sodium pyruvate. The experimental protocol was approved by the Ministero della salute (permit no. 815/2016-PR to M. Castagna).

Oocyte expression of KAAT1 WT and mutants

pSPORT-1 plasmid vector bearing KAAT1 wild type (WT), KAAT1-Flag [32] or the relative mutants were linearized by *Not1* digestion (Promega). Corresponding cRNAs were *in vitro* transcribed and capped using T7 RNA polymerase (Promega). Defolliculated oocytes were injected with 12.5 ng of cRNA dissolved in 50 nl of RNAse-free water via a manual microinjection system (Drummond). Before use, oocytes were maintained in Barth's solution at 16°C supplemented as described above.

Radiolabeled amino acid uptake in *Xenopus* oocytes

Amino acid uptake was evaluated 3 days after injection. Groups of 8–10 oocytes were incubated for 60 min in 120 μl of uptake solution (100 mM NaCl, 2 mM KCl, 1 mM $CaCl_2$, 1 mM $MgCl_2$, 5 mM HEPES/NaOH, pH 8) with 0.1 mM [^{3}H]-leucine (444 kBq/ml, specific activity 3.996 Tbq/mmol). Alternatively, to evaluate uptake induced in the presence of potassium ions, NaCl was substituted by 150 mM KCl. In the absence of Na^+, NaCl was replaced by choline chloride; in the absence of chloride, NaCl was replaced by sodium gluconate. In PGO (phenylglyoxal) experiments, oocytes were pretreated with 10 mM PGO for 60 min in the presence or in the absence of chloride, washed and then tested for uptake. In stereoselectivity experiments, uptake of [^{3}H]-L-leucine was measured in the presence of 4 mM unlabeled D-leucine. Uptake experiments were conducted at room temperature. After incubation oocytes were rinsed with ice cold wash solution (100 mM choline chloride, 2 mM KCl, 1 mM $CaCl_2$, 1 mM $MgCl_2$, 5 mM HEPES/choline hydroxide, pH 8), and dissolved in 250 μl of 10% SDS for liquid scintillation counting.

KAAT1-induced uptake was calculated as the difference between the mean uptake measured in cRNA injected oocytes and the mean uptake measured in non-injected oocytes. The statistical significance of the results was determined by student t-test.

Electrophysiological measurements

Currents generated by the transporters were recorded using the two-electrode voltage clamp (TEVC) technique (Warner oocytes clamp OC725 Warner Instruments, LLC1125 Dixwell Avenue Hamden, CT 06514 USA). The holding potential (V_h) was −60 mV and voltage pulses from −140 mV to +40 mV in 20 mV increments were applied for 200 ms. Clampex and Clampfit 10.2 Molecular Devices, (www.moleculardevices.com) were used to run the experiments, acquire and analyse the data, while Origin 8.0 (original Lab Corp., Northampton, MA, USA, www.originlab.com) for statistics and figures preparation. Transport currents were recorded only in oocytes expressing the KAAT1 WT or the indicated mutants and determined by subtracting the currents in the absence of organic substrate from those in its presence. The external control solution during the electrophysiological recordings had the following composition (mM): NaCl, 98; $MgCl_2$, 1; $CaCl_2$, 1.8, HEPES 5 mM. When necessary, NaCl was totally or partially substituted by TMACl, KCl or Na gluconate (in the presence of calcium lactate 10 mM). The final pH (7.6) was adjusted with NaOH, KOH, TMAOH respectively. The substrates, dissolved in water,

were added at 3 mM concentrations. Experiments were performed at room temperature (20–25 °C).

Chemiluminescence

To determine the surface expression of the transporter proteins, a FLAG epitope was inserted into the second extracellular loop of KAAT1, as described before [32]. The protein expression at the oocyte plasma membrane was evaluated by using the SOC (Single Oocyte Chemiluminescence). Oocytes expressing the KAAT1-flag WT or mutated transporter, as well as non-injected oocytes, were fixed with 4% paraformaldehyde in ND96. Then, they were rinsed for three times in cold ND96 for 5 min and, after 1h of incubation in blocking solution (BSA 1% + ND96 pH 7.6) they were incubated for 2h in primary mouse anti-flag antibody (SIGMA) at 1ug/mL concentration in 1% BSA-ND96 at 4°C. The oocytes were transferred at room temperature and kept for 1h in peroxidase-conjugated anti-mouse 1 ug/mL (www.jacksonimmune.com). Finally, each oocyte was transferred into a 96-well plate (Assay Plate White not treated flat bottom, Corning Costar, www.corning.com) and filled with 50uL SuperSignal Femto (Pierce, Euroclone, Milan, Italy www.euroclonegroup.it). Chemiluminescence was quantified with a Tecan Infinity 200 micro plate reader. The plates were read not later than 5 min after the transfer of the first oocyte. Results were normalized to the mean value obtained for the wild type flagged transporter for each batch.

Homology modeling

The outward-occluded model of *Manduca sexta* KAAT1 (Genbank accession AAC24190.1) based on the structure of LeuT (PDB code 2A65) was built using Nest [33]. The pairwise alignment between KAAT1 and LeuT was constructed using T-coffee [34] and refined according to the analysis of [35]. The two proteins exhibit ~25% sequence identity, suggesting a model of accuracy 1–2 Å in the Cα-atoms [36]. The side chains of non-conserved residues were optimized using SCAP [37]. The coordinates of the ligands were copied from those in the 2a65 template, with the exception of chloride, which was placed at the coordinates of the Glu 290 carboxyl C atom. Clashes between side chains were reduced by energy minimization using PLOP v15 [38]. The energy-minimized model contains 97.9% residues in favored and allowed regions of the Ramachandran plot, and only one residue, Val 207, from loop EL2, in a disallowed region. This overall procedure maintains fidelity to the backbone of LeuT, while producing reasonable side chain positions. The global ProQM score [39] of the model is 0.814, which is excellent, and on a par with that of the template (0.801).

RESULTS AND DISCUSSION

Ala 66 and Ser 68 of KAAT1 were mutated into the corresponding residues present respectively in the Na2 and Na1 sites of most NSS members, obtaining the A66G and S68A mutants (Fig. 1D). Thr 67 was substituted with glycine (T67G) and tyrosine (T67Y) to evaluate the effects of the elimination or increase of the side chain size, respectively.

The correct surface expression of the mutants was verified by chemiluminescence assay as reported in Fig. 2.

All the tested mutants showed a surface localization comparable to that of WT except for the A66G mutant, which was present at the plasma membrane at 80% of the WT value.

The mutant activity was analyzed by radiochemical assays measuring the uptake of 0.1 mM leucine in the presence of external 100 mM NaCl or 150 mM KCl and results are reported in Fig. 3. In the presence of a sodium gradient (Fig. 3A), A66G showed transport activity comparable to that of WT, whereas the S68A mutant activity was reduced to 58%; the substitution of Thr 67 with glycine reduced the transport activity by about 90%, whereas transport increased almost 1.5-fold in the T67Y mutant. A similar pattern was observed in the presence of 150 mM KCl (Fig. 3B): A66G showed transport activity comparable to that of the WT, while the T67Y activity was 2-fold that of the WT. The S68A mutant was inactive, as previously reported [25].

Transport currents in sodium solution recorded as the difference between the current measured in the presence of the substrate and that in its absence confirmed that the T67G mutant, although correctly localized in the membrane, is not functional (i.e., no currents were recorded in the presence of the indicated substrate, like non-injected oocytes [4]). For WT, A66G, and T67Y at a holding potential of −60 mV and in the presence of 1 mM leucine, an inward current of tens of nA was measured. For the S68A mutant however, previous observations were confirmed [25], specifically, leucine blocked a leak current in Na^+ buffer solution, revealing an apparently outwardly directed current (Fig. 4).

The mean values of transport currents were also measured at −140 mV, showing an increase relative to their values measured at −60 mV for WT, A66G, and T67Y, and for S68A as well, although in this case in the opposite direction. When the substrate was threonine, which has a lower apparent affinity for the WT protein [40], the transport current increased as expected for KAAT1 WT and for A66G at both potentials tested, although the increase for A66G was smaller than that observed for WT. Surprisingly, for T67Y (Fig. 4 inset) the threonine-induced current was lower than that induced by leucine at the same potential. The functionality and the ability to give rise to inwardly directed transport-associated currents was also verified for S68A, using threonine and proline (data not shown): these substrates elicited currents of hundreds of nA at −140 mV and about 60 nA at −60 mV.

To compare the substrate selectivity at different potentials, normalized currents were plotted as *I-V* curves. Again, the A66G behavior remained similar to that of WT KAAT1, the threonine-induced current being larger than the leucine-induced current only at −140 mV in potassium solution. In contrast, T67Y and S68A showed an altered current profile both in sodium and in potassium. T67Y exhibited a preference for leucine with sodium, and no preference with potassium as driver ion, moreover, the transport-associated current was greatly reduced when the driver ion was potassium. In S68A, threonine and proline were transported similarly (Fig. 5) whereas leucine, which has the highest affinity for WT in sodium [40,41], is transported by this mutant (Fig. 3A), except that the transport-associated current is outwardly directed, due to the strong reduction of the uncoupled sodium flux in the presence of this amino acid [42]. Interestingly, such a behavior is comparable with that of the mutant S308T [40] which is part of the substrate binding site [25] and with that of the

wild type when the driving ion is lithium [43]. Conversely in the presence of K^+ no current (Fig. 5) and no uptake (Fig. 3B) were recorded in the presence of this amino acid.

Although Gly 66, Thr 67, and Ser 68 do not directly contribute to the putative binding site for chloride, the paralogous CAATCH1 shares Gly 66, Thr 67, and Ser 68 with KAAT1, and is also weakly chloride dependent, suggesting that these residues may somehow contribute to this chloride sensitivity [2]. We therefore challenged the mutants in the absence of chloride by gluconate substitution. The chloride dependence of KAAT1 was not affected by modifications of Ala 66 and Ser 68 (Fig. 6A), whereas it was abolished when introducing a bulkier, polar residue like the aromatic tyrosine in the T67Y mutant. Considering the physico-chemical properties of the side chain of the native threonine, the modulation of the chloride dependence in this transporter seems therefore to be related to the size of the side chain of the residue in position 67. This observation agrees with the presence of a Phe residue in the same position in the Cl^--independent orthologue B^0AT1 [1,4,6]. Transport-associated currents measured in the presence of leucine and threonine for A66G and T67Y and in the presence of threonine and proline for the S68A mutant confirmed the uptake data (Fig. 6B).

As shown above, the T67Y mutant differentially altered the flux of sodium and of the amino acid; in fact, transport-associated currents were one tenth of those induced in KAAT1 WT, whereas leucine uptake increased 1.5-fold. Moreover, variable charge/amino acid coupling ratios have been reported previously for the WT in a manner that depends on the driving ion [43]. Therefore, changes in the charge:substrate ratio might also be expected for mutations that modify the ion-substrate interaction. The position corresponding to Thr 67 in TM1 was studied previously in the GABA transporter GAT1 [44], and was found to be involved in the switching between leak and coupled modes of transport. Specifically, the mutation of Tyr 60 in GAT1 to threonine induced an increase in lithium leak current and in the K_{05} for sodium of the substrate-coupled currents [44], i.e., the reverse of the behavior of KAAT1 T67Y. Notably, in T67Y the amino acid flux is strictly sodium dependent, as transport is completely abolished when choline replaces sodium in the uptake solution (Fig. 3A inset). This suggests that a conformation required for amino acid flux can be reached only in the presence of sodium or potassium as in the WT protein and that the substrate passes through the mutant protein (T67Y) by a mechanism that almost abolishes the sodium transport uncoupled currents [45], strongly reducing the ion flux (Fig. 4) relative to the wild type. This effect can be ascribed to the larger sidechain of tyrosine that could act as barrier to leaky ions. Moreover, the transport of Y67Y is not influenced by the presence of chloride (Fig. 6A) as revealed by the uptake measurements.

Molecular Dynamics simulations performed on the crystal structure of WT LeuT and E290S mutant [19,46], revealed a complex network of interactions that connects the sodium and chloride coordinating residues (or the negatively charged residue of the protein) with the extracellular gate of the transporter formed by Arg 30 and Asp 404 (corresponding to Arg 76 and Asp 460 in KAAT1). Specifically, the negative charge (Glu 290, in LeuT, or Cl^-) stabilizes Gln 250, which modulates its interaction with Arg 30, and in turn defines the formation of the Arg 30 – Asp 404 salt bridge, and thereby the closure of the extracellular pathway [19,46]. Exploiting the known sensitivity of KAAT1 Arg 76 to phenylglyoxal

(PGO) treatment [47], we tested whether chloride can influence the interaction of Arg 76 with PGO, and thereby reveal a chloride-induced modification of the access at the putative extracellular gate of KAAT1. As reported in Fig. 7, 10 mM PGO treatment in the absence of chloride caused a reduction of leucine uptake to 31% of the control condition for KAAT1 WT, confirming the possibility that Arg 76 reacts with the chemical agent. Interestingly, in the presence of chloride, WT KAAT1 was more sensitive to PGO inhibition (residual uptake of 15 % of control condition) indicating an increased reactivity of Arg 76 likely due to the opening of the extracellular gate of the transporter promoted by chloride and a resultant increase in accessibility of Arg 76 to PGO. Confirming the chloride independence of the T67Y mutant, its interaction with PGO was significantly less influenced by the presence of the anion (Fig. 7). These results are consistent with the presence of a complex network of interactions connecting the Na1 and Cl^- coordinating residues to the extracellular gate of the transporter, as identified in WT LeuT and E290S mutant [19,46]. Moreover, the observed effects on Na^+ and Cl^- interaction in the T67Y mutant indicate that this residue may participate in, or indirectly influence, this network in KAAT1.

In the serotonin transporter SERT the residue corresponding to Thr 67, Tyr 95, influences the discrimination between R- and S-citalopram, indicating a role in the stereo selectivity of antagonists [48]. Many insect transporters can transport not only proteinogenic L-amino acids but also their corresponding D-enantiomers [49,50]. KAAT1 is not stereoselective, although in physiological conditions (i.e., K solution) it will preferentially transport L-amino acids [51,52]. To assess whether position 67 influences stereo-selectivity, we performed competition experiments in which the uptake of 0.1 mM [^{3}H]-L-leucine in the presence of 100 mM NaCl was challenged by the application of 4 mM unlabeled D-leucine. In these conditions, the residual uptake activity of the wild type protein was about 20% of control (Fig. 8A) whereas that of the T67Y mutant was 65% of control. Transport currents confirmed the ability of the WT to transport D-leucine and the preference for L-leucine of the T67Y mutant (Fig. 8B). These data therefore show that T67Y has altered stereoselectivity.

In LeuT, the residue corresponding to KAAT1 Thr 67 is Asn 21, which lines the substrate binding site and also apparently provides a hydrogen-bonding acceptor which may help stabilize the side chain of Ser 256, which in turn, provides a hydrogen-bond acceptor for the substrate amine nitrogen atom (Fig. 1B). Accordingly, our data indicate that the substitution of Thr 67 in KAAT1 not only modifies the substrate selectivity so that the T67Y mutant favors leucine in any tested condition (Fig. 5), but also alters the stereoselectivity of the transporter.

While in SERT the residue is important particularly for the interaction with antagonist ligands, for KAAT1 the role exerted by Thr 67 is different: it defines substrate specificity by enabling the protein to translocate also D-amino acids [51,52]. The physiological significance of the ability of KAAT1 to import D-amino acids is still unknown, but it is common for insects to carry out this kind of uptake and to exploit D-amino acids as regulatory molecules [50].

CONCLUSION

Taken as a whole, our data support the hypothesis that assigns an important role to Thr 67 in the function of KAAT1: mutating this residue we were able to influence most aspects of the transport process. Thr 67 appears to be involved in the mechanism that realizes the coupling between driven and driver fluxes, in the Cl^- interaction, and in substrate recognition. These roles are consistent with the structural data for LeuT [7,19] and recently obtained for SERT [11], where the residue corresponding to Thr 67 either appears to stabilize the substrate amine group, as in Asn 21 of LeuT, or forms the base of the substrate binding site, reaching over to hydrogen-bond with the backbone of TM6, as in Tyr 95 of SERT (Fig. 1D). The fact that Thr 67 is sandwiched between the Na1 and Na2 binding site and residues Gly 20/Gly 94 and Ala 22/Ala 96 (in LeuT/SERT, respectively) provides a connection between the driving ions and the substrate binding site, and beyond that, through Na1 to the chloride binding site.

ACKNOWLEDGEMENTS

This work was supported by University Research Program 2008 to M.C., PUR (University Research Program)-Università degli Studi di Milano 2008 to M.C., by Fondazione comunitaria del Varesotto ONLUS, (152/2015) and FAR (Fondo di Ateneo per la Ricerca)- Università dell' Insubria to E.B. and by the Division of Intramural Research of the NIH, National Institute of Neurological Disorders and Stroke to L.R.F.

ABBREVIATIONS:

CAATCH1	Cation Anion activated Amino acid Transporter/Channel 1
KAAT1	K^+-coupled Amino Acid Transporter 1
DAT	dopamine transporter
SERT	serotonin transporter
GAT1	GABA transporter GAT1
TM	transmembrane domain
TMA	tetramethylammonium

REFERENCES

[1]. Broer S, The SLC6 orphans are forming a family of amino acid transporters, Neurochem Int, 48 (2006) 559–567. [PubMed: 16540203]

[2]. Bettè S, Castagna M, Bossi E, Peres A, Sacchi VF, The SLC6/NSS family members KAAT1 and CAATCH1 have weak chloride dependence, Channels (Austin), 2 (2008) 358–362. [PubMed: 19066444]

[3]. Boudko DY, Molecular basis of essential amino acid transport from studies of insect nutrient amino acid transporters of the SLC6 family (NAT-SLC6), J Insect Physiol. 4 (2012) 433–449.

[4]. Margheritis E, Terova G, Cinquetti R, Peres A, Bossi E, Functional properties of a newly cloned fish ortholog of the neutral amino acid transporter B0AT1(SLC6A19), Comp Biochem Physiol A Mol Integr Physiol. 2 (2013) 285–92.

[5]. Meleshkevitch EA, Voronov DA, Miller NM, Penneda M, Fox JM, Metzler R, Boudko DY, A novel eukaryotic Na^+ methionine selective symporter is essential for mosquito development, Insect Biochem Mol Biol. 43(2013) 755–67. [PubMed: 23748165]

[6]. Margheritis E, Imperiali FG, Cinquetti R, Vollero A, Terova G, Rimoldi S, Girardello R, Bossi E, Amino acid transporter $B^{(0)}$AT1 (SLC6A19) and ancillary protein: impact on function, Pflugers Arch. 468 (2016) 1363–74. [PubMed: 27255547]

[7]. Yamashita A, Singh SK, Kawate T, Y Jin E Gouaux, Crystal structure of a bacterial homologue of Na^+/Cl^--dependent neurotransmitter transporters, Nature. 437 (2005) 215–223. [PubMed: 16041361]

[8]. Penmatsa A, Wang KH, Gouau E, X-ray structure of dopamine transporter elucidates antidepressant mechanism, Nature. 503 (2013) 85–90. [PubMed: 24037379]

[9]. Penmatsa A, Wang KH, Gouaux E, X-ray structures of Drosophila dopamine transporter in complex with nisoxetine and reboxetine, Nat Struct Mol Biol. 22(2015) 506–508 [PubMed: 25961798]

[10]. Wang KH, Penmatsa A, Gouaux E, Neurotransmitter and psychostimulant recognition by the dopamine transporter, Nature. 521 (2015) 322–327. [PubMed: 25970245]

[11]. Coleman JA, Green EM, Gouaux E, X-ray structures and mechanism of the human serotonin transporter, Nature. 532 (2016) 334–9. [PubMed: 27049939]

[12]. Khafizov K, Perez C, Koshy C, Quick M, Fendler K, Ziegler C, Forrest LR, Investigation of the sodium-binding sites in the sodium-coupled betaine transporter BetP, Proc Natl Acad Sci U S A. 109(2012) E3035–3044. [PubMed: 23047697]

[13]. Abramson J, Wright EM, Structure and function of $Na^{(+)}$-symporters with inverted repeats, Curr Opin Struct Biol. 19 (2009) 425–32. [PubMed: 19631523]

[14]. Focke PJ, Wang X, Larsson HP, Neurotransmitter transporters: structure meets function, Structure. 21 (2013) 694–705. [PubMed: 23664361]

[15]. Forrest LR, Tavoulari S, Zhang YW, Rudnick G, Honig B, Identification of a chloride ion binding site in Na^+/Cl^--dependent transporters, Proc Natl Acad Sci U S A. 104 (2007) 12761–12766. [PubMed: 17652169]

[16]. Zomot E, Bendahan A, Quick M, Zhao Y, Javitch JA, Kanner BI, Mechanism of chloride interaction with neurotransmitter:sodium symporters, Nature. 449 (2007) 726–730. [PubMed: 17704762]

[17]. Kanner BI, Molecular physiology: intimate contact enables transport, Nature. 437 (2005) 203–205. [PubMed: 16148921]

[18]. Tavoulari S, Rizwan AN, Forrest LR, Rudnick G, Reconstructing a chloride-binding site in a bacterial neurotransmitter transporter homologue, J. Biol Chem. 286 (2011) 2834–2842. [PubMed: 21115480]

[19]. Kantcheva AK, Quick M, Shi L, Winther AM, Stolzenberg S, Weinstein H, Javitch JA, Nissen P, Chloride binding site of neurotransmitter sodium symporters, Proc Natl Acad Sci U S A. 110 (2013) 8489–8494. [PubMed: 23641004]

[20]. Castagna M, Shayakul C, Trotti D, Sacchi VF, Harvey WR, Hediger MA. Cloning and characterization of a potassium-coupled amino acid transporter, Proc. Natl. Acad. Sci. U S A 95 (1998) 5395–5400. [PubMed: 9560287]

[21]. Soragna A, Mari SA, Pisani R, Peres A, Castagna M, Sacchi VF, et al. Structural domains involved in substrate selectivity in two neutral amino acid transporters. Am. J. Physiol. Cell. Physiol 287 (2004) C754–C761. [PubMed: 15140745]

[22]. Feldman DH, Harvey WR, Stevens BR, A novel electrogenic amino acid transporter is activated by K+ or Na+, is alkaline pH-dependent, and is Cl—independent, J. Biol. Chem 275 (2000) 24518–24526. [PubMed: 10829035]

[23]. Rudnick G, Structure/function relationships in serotonin transporter: new insights from the structure of a bacterial transporter, Handb Exp Pharmacol. 175 (2006) 59–73.

[24]. Billesbølle CB, Mortensen JS, Sohail A, Schmidt SG, Shi L, Sitte HH, Gether U, Loland CJ, Transition metal ion FRET uncovers $K^{(+)}$ regulation of a neurotransmitter/sodium symporter. Nat Commun. (2016) doi:10.1038/ncomms12755.

[25]. Castagna M, Bossi E, Sacchi VF, Molecular physiology of the insect K-activated amino acid transporter 1 (KAAT1) and cation-anion activated amino acid transporter/channel 1 (CAATCH1) in the light of the structure of the homologous protein LeuT, Insect Mol. Biol 18 (2009) 265–279. [PubMed: 19389142]

[26]. Zhou Y, Zomot E, Kanner BI, Identification of a lithium interaction site in the gamma-aminobutyric acid (GABA) transporter GAT-1, J Biol Chem. 281 (2006) 22092–22099. [PubMed: 16757479]

[27]. Borre L, Andreassen TF, Shi L, Weinstein H, Gether U, The second sodium site in the dopamine transporter controls cation permeation and is regulated by chloride, J Biol Chem. 289 (2014) 25764–25773. [PubMed: 25063810]

[28]. Camargo SM, Makrides V, Virkki LV, Forster IC, Verrey F, Steady-state kinetic characterization of the mouse $B^{(0)}$AT1 sodium-dependent neutral amino acid transporter, Pflugers Arch. 451 (2005) 338–348. [PubMed: 16133263]

[29]. Böhmer C, Bröer A, Munzinger M, Kowalczuk S, Rasko JE, Lang F, Bröer S, Characterization of mouse amino acid transporter B0AT1 (SLC6A19), Biochem J.389(2005) 745–751. [PubMed: 15804236]

[30]. Mari SA, Soragna A, Castagna M, Bossi E, Peres A, Sacchi VF, Aspartate 338 contributes to the cationic specificity and to driver-amino acid coupling in the insect cotransporter KAAT1, Cell. Mol. Life Sci. 61 (2004) 243–256. [PubMed: 14745502]

[31]. Castagna MM, Soragna AA, Mari SA, Santacroce M, Bettè S, Mandela PG, et al., Interaction between lysine 102 and aspartate 338 in the insect amino acid cotransporter KAAT1, Am. J. Physiol. Cell. Physiol. 293 (2007) C1286–C1295. [PubMed: 17626242]

[32]. Giovanola M, D'Antoni F, Santacroce M, Mari SA, Cherubino F, Bossi E, Sacchi VF, Castagna M, Role of a conserved glycine triplet in the NSS amino acid transporter KAAT1, Biochim Biophys Acta. 1818 (2012) 1737–1744. [PubMed: 22402268]

[33]. Petrey D, Xiang Z, Tang CL, Xie L, Gimpelev M, Mitros T, et al., Using multiple structure alignments, fast model building, and energetic analysis in fold recognition and homology modelling, Proteins 53 (2003) 430–435. [PubMed: 14579332]

[34]. Notredame C, Higgins DJ, Heringa J, T-Coffee: A novel method for fast and accurate multiple sequence alignment, J.Mol. Biol 302 (2000) 205–217. [PubMed: 10964570]

[35]. Beuming T, Shi L, Javitch JA, Weinstein H, A comprehensive structure-based alignment of prokaryotic and eukaryotic neurotransmitter/Na+ symporters (NSS) aids in the use of the LeuT structure to probe NSS structure and function, Mol. Pharmacol 70 (2006) 1630–42. [PubMed: 16880288]

[36]. Olivella M, Gonzalez A, Pardo L, Deupi X, Relation between sequence and structure in membrane proteins, Bioinformatics 29 (2013) 1589–1592. [PubMed: 23677941]

[37]. Xiang Z, Honig B, Extending the accuracy limits of prediction for side-chain conformations, J Mol Biol 311 (2001) 421–430. [PubMed: 11478870]

[38]. Jacobson MP, Friesner RA, Xiang Z, Honig B, On the role of the crystal environment in determining protein side-chain conformations, J Mol Biol. 320 (2002) 597–608. [PubMed: 12096912]

[39]. Ray A, Lindahl E, Wallner B. Model quality assessment for membrane proteins, Bioinformatics 26 (2010) 3067–3074. [PubMed: 20947525]

[40]. Miszner A, Peres A, Castagna M, Betté S, Giovannardi S, Cherubino F, et al., Structural and functional basis of amino acid specificity in the invertebrate cotransporter KAAT1, J. Physiol 58 (2007) 1899–1913.

[41]. Peres A, Selectivity: a sticky affair, Physiology News 70 (2008) 18–20

[42]. Nelson N, Sacher A, Nelson H, The significance of molecular slips in transport systems, Nat Rev Mol Cell Biol. 11 (2002) 876–881.

[43]. Bossi E, Vincenti S, Sacchi VF, Peres A, Simultaneous measurements of ionic currents and leucine uptake at the amino acid cotransporter KAAT1 expressed in Xenopus laevis oocytes, Biochim. Biophys. Acta 1495 (2000) 34–39. [PubMed: 10634930]

[44]. Kanner BI, Transmembrane domain I of the gamma-aminobutyric acid transporter GAT-1 plays a crucial role in the transition between cation leak and transport modes, J Biol Chem. 278 (2003) 3705–3712. [PubMed: 12446715]

[45]. Andrini O, Ghezzi C, Murer H, Forster IC, The leak mode of type II Na(+)-P(i) cotransporters, Channels 2 (2008) 346–357. [PubMed: 18989094]

[46]. Tavoulari S, Margheritis E, Nagarajan A, DeWitt DC, Zhang YW, Rosado E, Ravera S, Rhoades E, Forrest LR, Rudnick G, Two Na+ Sites Control Conformational Change in a Neurotransmitter Transporter Homolog, J Biol Chem. 291 (2016) 1456–1471. [PubMed: 26582198]

[47]. Castagna M, Vincenti S, Marciani P, Sacchi VF, Inhibition of the lepidopteran amino acid co-transporter KAAT1 by phenylglyoxal: role of arginine 76, Insect Mol Biol. 11 (2002) 283–289. [PubMed: 12144692]

[48]. Henry LK, Field JR, Adkins EM, Parnas ML, Vaughan RA, Zou MF et al., Tyr-95 and Ile-172 in transmembrane segments 1 and 3 of human serotonin transporters interact to establish high affinity recognition of antidepressants, J Biol Chem. 281 (2006) 2012–23. [PubMed: 16272152]

[49]. Geer BW, Utilization of D-amino acids for growth by Drosophila melanogaster larvae, J Nutr, 90 (1966) 31–39. [PubMed: 5918848]

[50]. Miller MM, Popova LB, Meleshkevitch EA, Tran PV, Boudko DY, The invertebrate B(0) system transporter, D. melanogaster NAT1, has unique d-amino acid affinity and mediates gut and brain functions, Insect Biochem Mol Biol. 38 (2008) 923–931. [PubMed: 18718864]

[51]. Vincenti S, Castagna M, Peres A, Sacchi VF, Substrate selectivity and pH dependence of KAAT1 expressed in Xenopus laevis oocytes, J Membr Biol. 174 (2000) 213–224. [PubMed: 10758175]

[52]. Vollero A, Imperiali FG, Cinquetti R, Margheritis E, Peres A, Bossi E, The D-amino acid transport by the invertebrate SLC6 transporters KAAT1 and CAATCH1 from Manduca sexta, Physiol Rep. 2016 doi:10.14814/phy2.12691.

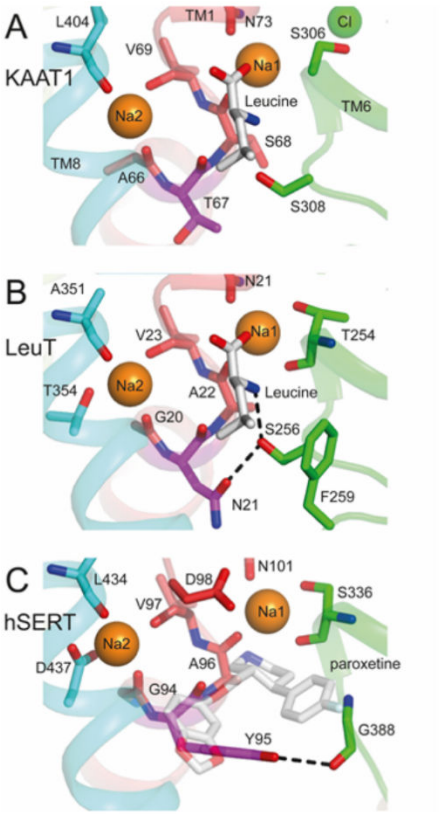

D

```
KAAT1      NNIEFLMSCIATSVGLGNVWRFPFIAYQ 83
CAACHT1    NNIEFLMSCIATSVGLGNVWRFPFIAYQ 83
LeuTAa     TRLGLILAMAGNAVGLGNFLRFPVQAAE 37
DATcryst   GKVDFLLSVIGFAVDLANVWRFPYLCYK 40
TnaT       SRSGFIFATIGAAVGLGNFWRFPFMAYQ 37
TyT1       SKIGFILTCVGSAVGMANIWAFPYRVGK 37
hB0AT1     NKAQYMLTCLGFCVGLGNVWRFPYLCQS 64
hGAT-1     GRFDFLMSCVGYAIGLGNVWRFPYLCGK 76
hGAT-2     HKMEFVLSVAGEIIGLGNVWRFPYLCYK 46
hGAT-3     NKVEFVLSVAGEIIGLGNVWRFPYLCYK 82
hGLYT-2    SKLDFILSMVGYAVGLGNVWRFPYLAFQ 223
hPROT      GKLDFLLSCIGYCVGLGNVWRFPYRAYT 69
hSERT      KKVDFLLSVIGYAVDLGNVWRFPYICYQ 111
hDAT       KKIDFLLSVIGFAVDLANVWRFPYLCYK 92
hCREAT-1   RQMDFIMSCVGFAVGLGNVWRFPYLCYK 84
hTAUT      SKIDFVLSVAGGFVGLGNVWRFPYLCYK 73
```

Fig. 1.

A, B, C, Structure of regions corresponding to Thr 67 in KAAT1, LeuT and hSERT. The predicted binding site region in the homology model of msKAAT1 (A) is compared to the sites in LeuT (PDB code 2A65) and hSERT (PDB code 5I6X, with Na2 from PDB entry 5I71). Thr 67 is shown using purple sticks, and other notable binding site residues are shown as sticks using the colors of the helices to which they belong: TM1 (red), TM6 (green), and TM8 (cyan), shown also in cartoon representation. Bound amino acid leucine and paroxetine are shown as gray sticks and paroxetine is semi-transparent, for clarity. Sodium (orange) and chloride ions, where present (green), are shown as spheres. Probable hydrogen-bonds mentioned in the main text are indicated with dashed black lines. For all groups, oxygen and nitrogen atoms are colored red and blue, respectively. A few binding site residues have been omitted for clarity. D, Alignment of transmembrane domain I of some NSS members highlighting Thr 67 of KAAT1 and the corresponding residues in the other proteins.

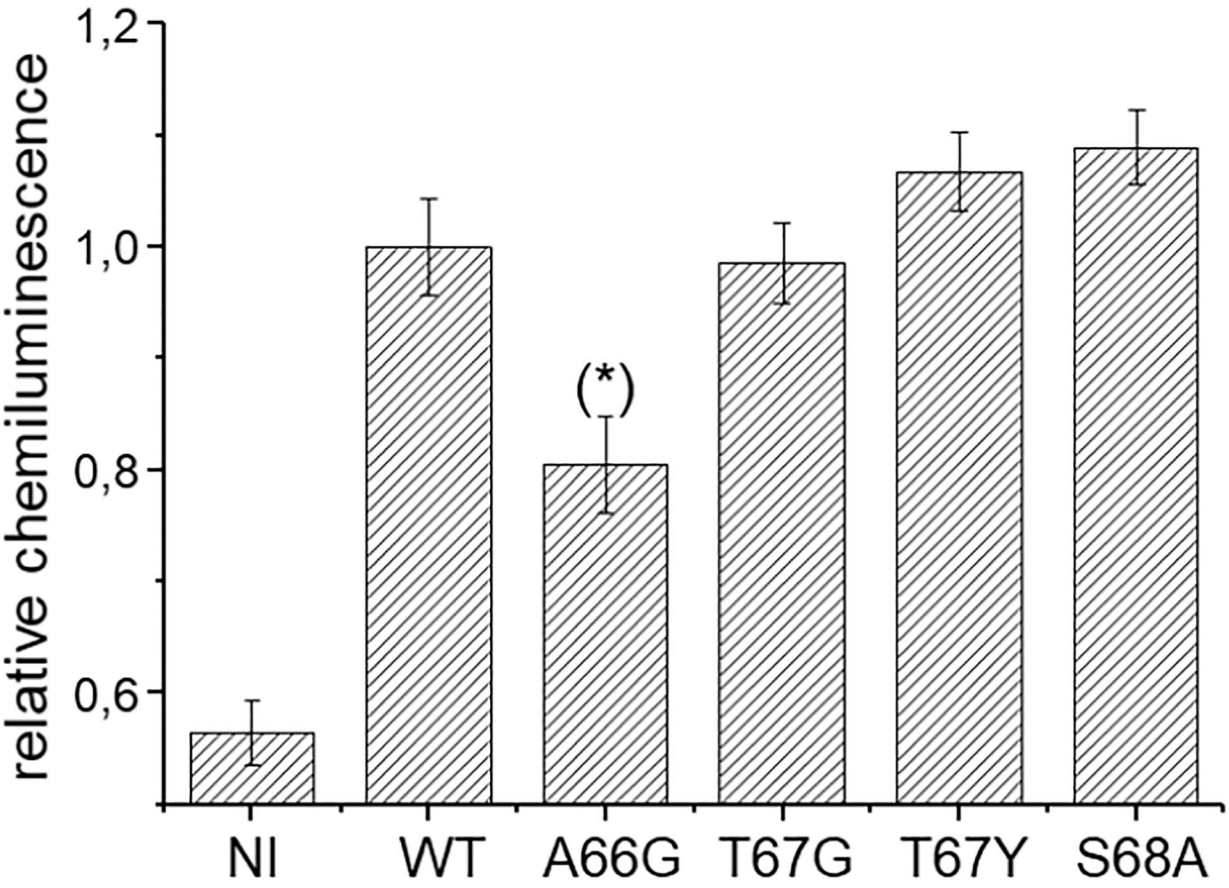

Fig. 2.

Surface expression of FLAG-tagged KAAT1 WT and mutants. Oocytes expressing the wild-type or the indicated mutants of KAAT1-FLAG were secondarily labelled with peroxidase-conjugated goat anti-mouse (IgG-HRP) after exposure to mouse anti FLAG. The chemiluminescence was detected from 38–80 oocytes from 3 different batches (NI:n=85;WT:n=54; A66G:n=55; T67G:n=38; T67Y:n=50; S68A:n= 38). The data were normalized to the mean value of the wild-type KAAT1 FLAG of each batch. (*) Statistically significant, $P<0.05$, when compared to all the other transporter expressing condition.

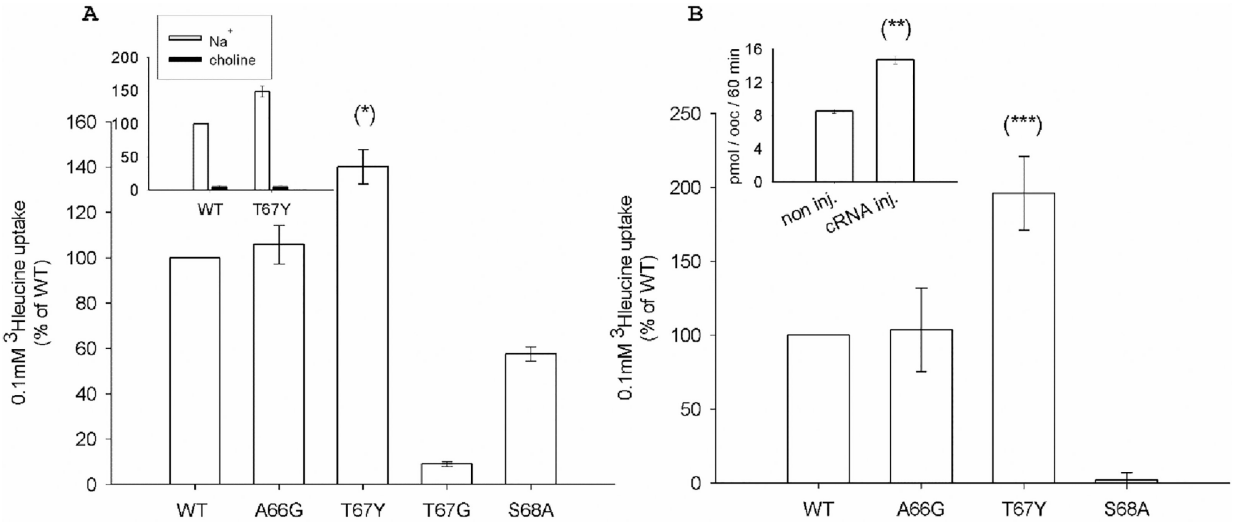

Fig. 3.

Ion dependence of 0.1 mM leucine uptake induced by KAAT1 WT and mutants. Data are means ± S.E. of three independent experiments with n ranging from 30 to 40, and are expressed as percentage of the WT induced uptake. (A): Uptake measured in the presence of 100 mM NaCl. Insert: Na^+-dependence of KAAT1 induced uptake. In the absence of Na^+, osmolarity was maintained substituting NaCl with choline chloride. (B) Uptake measured in the presence of 150 mM KCl. Insert: uptake measured in non-injected oocytes or in oocytes injected with KAAT1 WT cRNA. Data are means ± SE of a representative experiment with n ranging from 10 to4. (*), (***) Statistically significant, P<0.01 when compared with WT or other mutants in the same condition; (**) Statistically significant, P<0.001 when compared with non-injected oocytes.

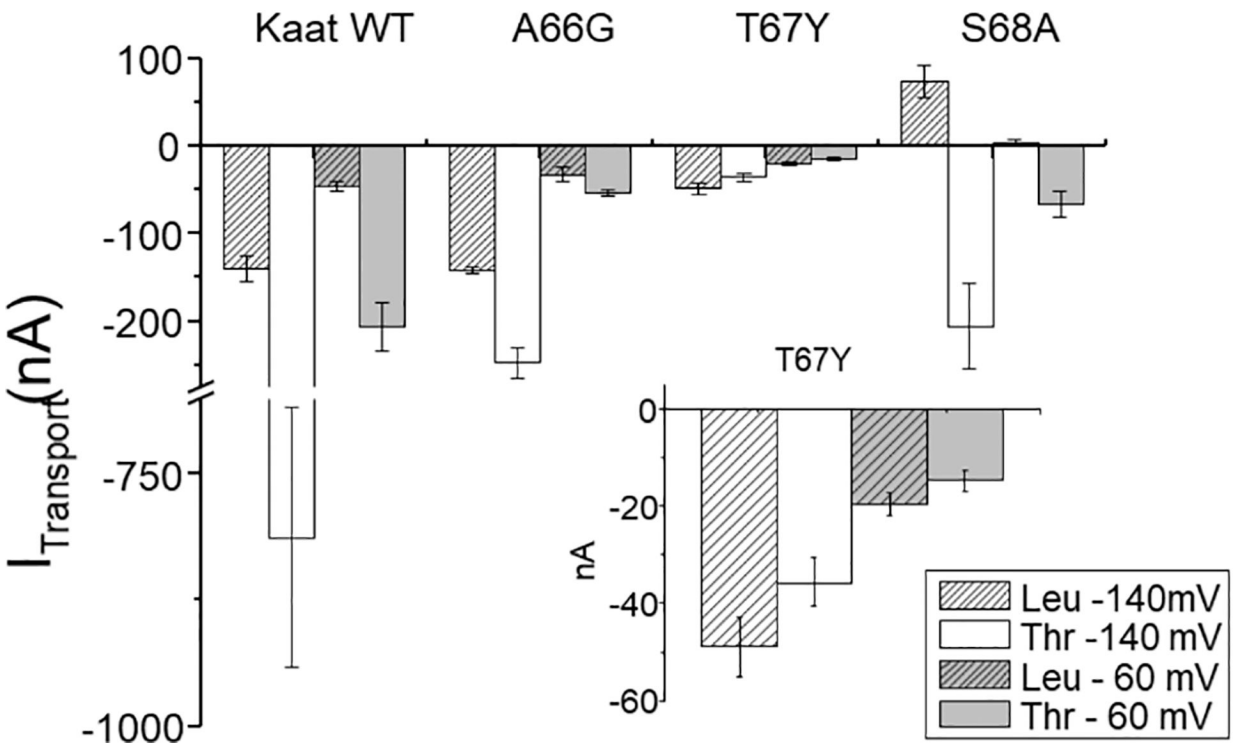

Fig. 4.

Transport associated currents. Means of the transport currents recorded at −140 mV and at −60 mV in the presence of threonine (3 mM) or leucine (1 mM). Values are means ± s.e.m. from several oocytes (n = from 4 to 25) heterologously expressing KAAT1 WT or the indicated mutants, and with Na^+ as driving ion (sodium buffer solution pH 7.5). In the inset the currents generated by T67Y are enlarged, to highlight the reduced currents recorded in threonine. For S68A currents were measured also in the presence of proline (–307.45 ± 91.07 nA at −140 mV and −67.60 ± 20.77 nA at −60 mV; data not reported in the histograms).

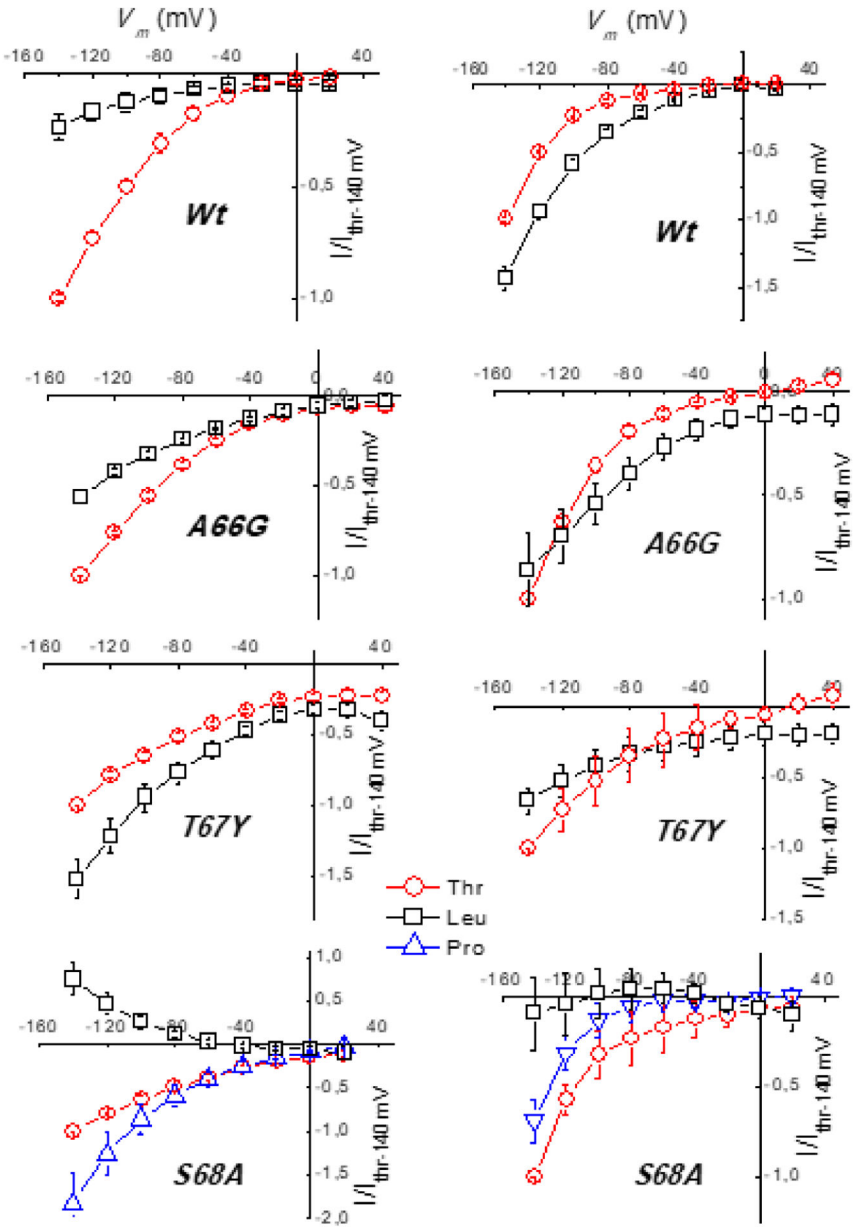

Fig. 5.

Current-Voltage relationships of normalized currents. Sodium (left) or potassium buffer solution (right) at pH 7.6 in the presence of threonine and leucine (proline only for S68A). Data were obtained by subtracting the traces recorded in the absence of the indicated substrate from those recorded in its presence, and normalized to the mean value in threonine at −140 mV for each batch before averaging. Values are means ± SE from several oocytes (n = from 4 to 20) in each tested group. Currents were recorded as described in Materials and Methods.

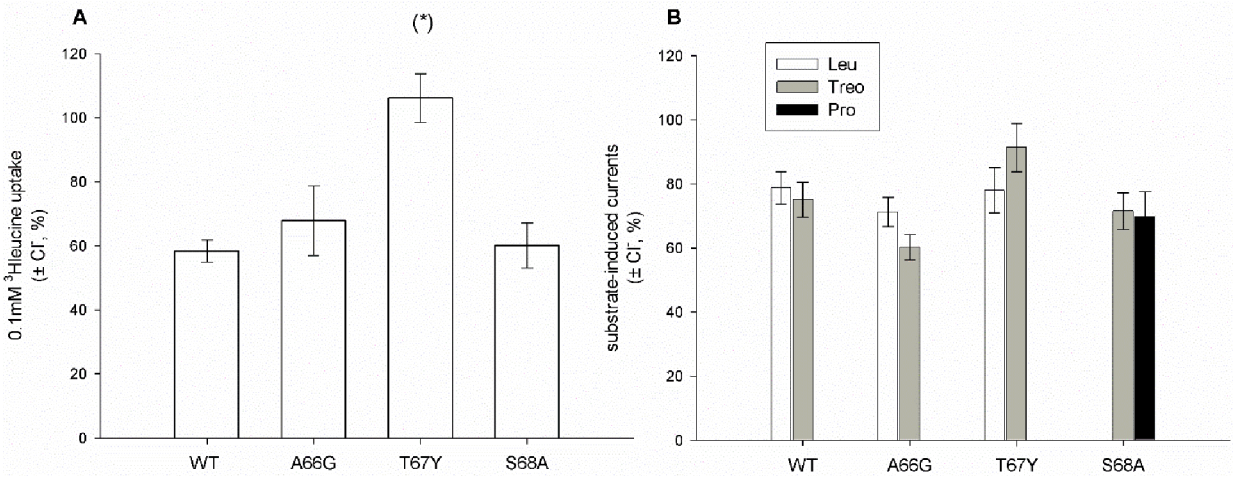

Fig. 6.

Chloride dependence of the transport activity of KAAT1 WT and mutants. (A) Uptake of 0.1mM leucine in the absence of chloride was measured substituting 100 mM NaCl with 100 mM sodium gluconate. Data are expressed as percentage of the uptake measured in control conditions (i.e. in the presence of 100 mM NaCl) and are means ± S.E of three independent experiments with n ranging from 30 to 40. (*) Statistically significant, $P<0.001$ when compared with WT or other mutants. (B) Transport-associated current recorded at −60 mV in the presence of leucine, threonine, or proline (only for S68A), in the absence of chloride (substituted by sodium gluconate), expressed as percentage of the currents measured in the control condition (presence of chloride). Data are the means ± S.E from 3 different experiments with n ranging from 3 to 15, according to the different condition.

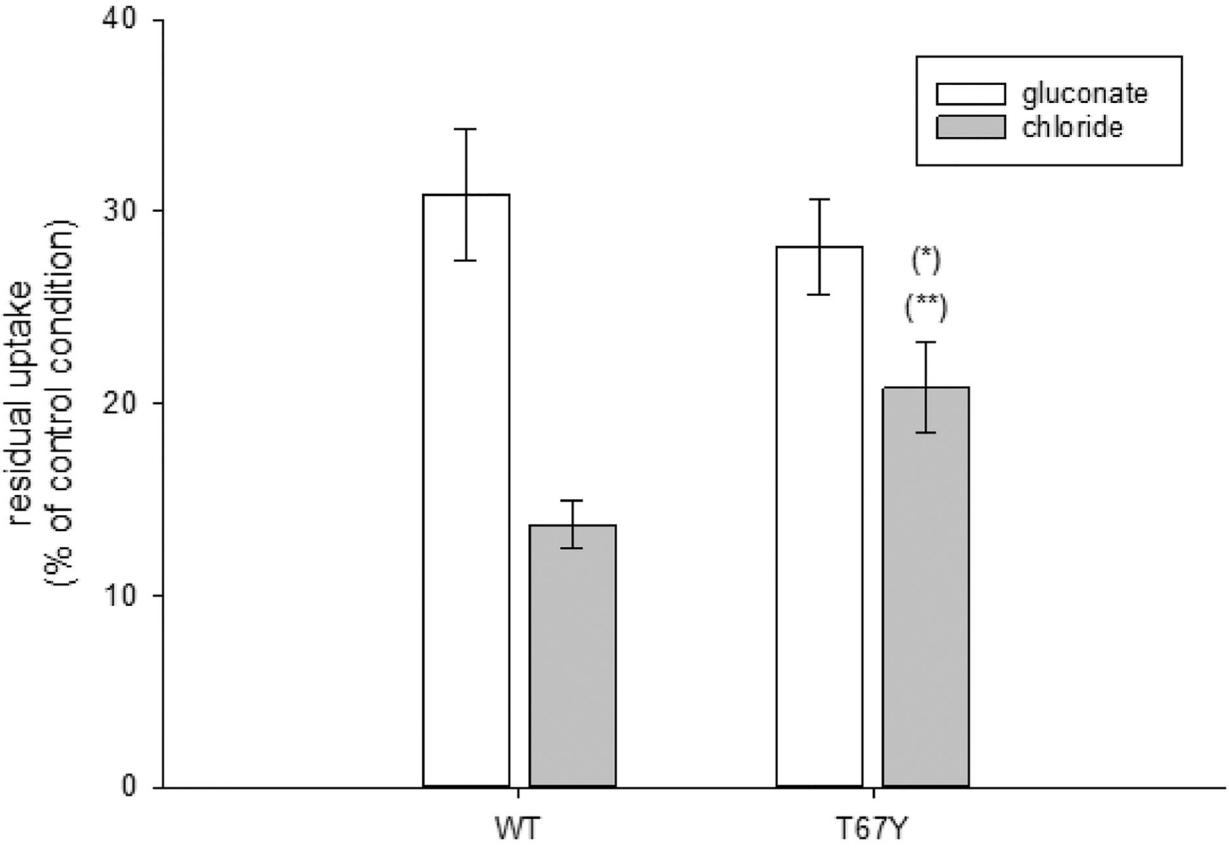

Fig. 7.

Effects of 10 mM PGO (phenylglyoxal) treatment. Leucine uptake was measured before and after treatment with 10 mM PGO conducted in the presence of 100 mM NaCl or 100 mM sodium gluconate. Data are expressed as percentage of the uptake measured in control conditions (i.e. in the absence of PGO) and are means ± S.E of three independent experiments with n ranging from 30 to 40. (*) Statistically significant, $P<0.03$ when compared with gluconate condition; (**) Statistically significant, $P< 0.01$ when compared with WT treated in the presence of chloride.

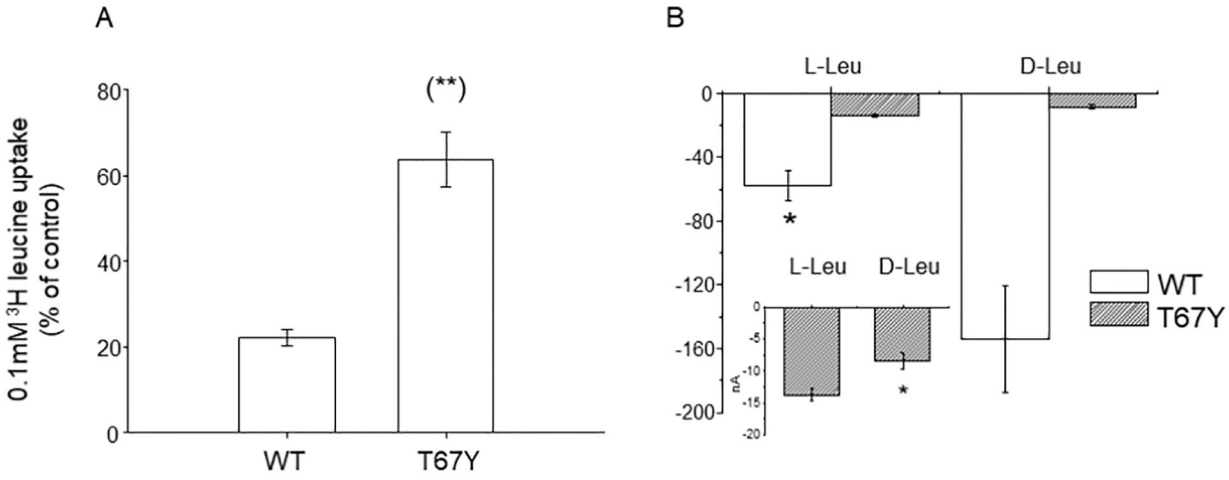

Fig. 8.

Effects of D-leucine application on L-leucine uptake. A) 0.1mM [^{3}H]-L-leucine uptake induced by KAAT1 WT and the T67Y mutant was measured in the absence or in the presence of 4 mM unlabeled D-leucine. Data are means ± S.E. of three independent experiments with n ranging from 30 to 40 and are expressed as percentage of control uptake. (**) Statistically significant, $P<0.001$ when compared with WT. B) Transport current in the presence of D- and L- leucine reported as raw mean values ± SEM for WT (n = 25) and for T67Y (n = 7). The currents recorded in the presence of D-leucine are larger than the currents recorded in L-leucine for the wild type, while the opposite is true for the T67Y mutant. The inset is an enlargement of the data for T67Y (*0.05 level one-way ANOVA).